AIP | Journal of Applied Physics

Synthesis, characterizations, and field emission studies of crystalline Na2V6O16 nanobelt paper

S. H. Lim, J. Y. Lin, Y. W. Zhu, C. H. Sow, and W. Ji

Citation: J. Appl. Phys. 100, 016105 (2006); doi: 10.1063/1.2213186
View online: http://dx.doi.org/10.1063/1.2213186
View Table of Contents: http://jap.aip.org/resource/1/JAPIAU/v100/i1
Published by the AIP Publishing LLC.

Synthesis, characterizations, and field emission studies of crystalline $Na_2V_6O_{16}$ nanobelt paper

S. H. Lim and J. Y. Lin[a)]
Institute of Chemical and Engineering Sciences, Singapore 627833, Singapore

Y. W. Zhu, C. H. Sow, and W. Ji
Department of Physics, National University of Singapore, Singapore 117542, Singapore and Nanoscience and Nanotechnology Initiative, National University of Singapore, Singapore 117542, Singapore

(Received 4 December 2005; accepted 15 May 2006; published online 12 July 2006)

Crystalline $Na_2V_6O_{16}\cdot 3H_2O$ nanobelts have been synthesized by refluxing V_2O_5 and NaF and self-weaved into a sheet of paper via a vacuum filtration process. Scanning electron microscopy, x-ray diffraction, and x-ray photoelectron spectroscopy were used to characterize the morphology, structure, and chemical composition of the nanobelt papers. The dehydrated $Na_2V_6O_{16}$ nanobelts are excellent field emission candidates, with a low turn-on field of 6.8 V/μm, a large current density up to 2.5 mA/cm^2 at an electric field of 10 V/μm, and a very uniform distribution of emission sites.
 [DOI: 10.1063/1.2213186]

Carbon nanotubes (CNTs) have been identified as a promising field emission (FE) electron source[1] due to its good thermal stability, low operation voltage, and high emission current. On the other hand, some noncarbonaceous nanomaterials, such as metal oxide,[2–5] sulphide,[6,7] and silicide[8] nanowires or nanobelts, may also deliver relatively uniform and stable FE currents, thereby expanding the pool of candidates for field emitters.

In this work, we report the synthesis, characterization, and field emission studies of multicomponent $Na_2V_6O_{16}\cdot 3H_2O$ crystalline nanobelts. This is motivated by the unique morphology of individual nanobelts which have sharp corners and edges of nanobelts and are assumed to contribute to high emission current.[5]

The $Na_2V_6O_{16}$ nanobelts were prepared using a hydrothermal method.[9] Sodium fluoride (NaF, Merck >99%) and vanadium pentoxide (V_2O_5, Sigma-Aldrich >99%) (1:5 weight ratio, respectively) were refluxed for 24 h at 180 °C. After that, the obtained nanobelts were vacuum filtered, rinsed with distilled water, and then air dried at 80 °C overnight. The $Na_2V_6O_{16}$ nanobelts were self-weaved into a sheet of paper (same size as the filter paper) and could be peeled off easily from the filter paper for the subsequent characterizations and field emission measurements.

Figure 1(a) is the scanning electron microscopy (SEM, JEOL 6400F) image of the dehydrated $Na_2V_6O_{16}$ nanobelts, which were air annealed at 300 °C for 2 h. It can be seen that the nanobelts have a typical length of tens micrometers and a width ranging from 50 to 140 nm. The thickness of the nanobelts was estimated to be ~5 nm. The randomly crisscrossing of long nanobelts might be responsible for their self-weaving actions into a paper.

As shown in Fig. 1(b) [x-ray diffraction (XRD), Bruker 8D Advance with Cu $K\alpha$ radiation], the observed XRD peaks can be readily indexed to a pure monoclinic crystalline phase of $Na_2V_6O_{16}\cdot 3H_2O$ structures (Barnesite, JCPDS No. 16-601), which is a member of the Hewettite family ($M_2V_6O_{16}\cdot nH_2O$, M=monovalent element or $MV_6O_{16}\cdot nH_2O$, M=divalent).

The core-level V2p, O1s, Na2p, and valence bands (VB, Fig. 2) of bulk V_2O_5 and $Na_2V_6O_{16}$ nanobelts were investigated using x-ray photoelectron spectroscopy [XPS, ESCA MK II using Mg $K\alpha$ (1254.6 eV) source]. The core-level peaks (not shown here) corresponding to V2$p_{3/2}$ at 517.2 eV (characteristic of a pentavalent V^{5+} state), V2$p_{1/2}$ at 524.6 eV, and O1s at 530.0 eV were similar for bulk V_2O_5 and $Na_2V_6O_{16}$ nanobelts. However, the Na2p peak at ~30 eV was observed only for the $Na_2V_6O_{16}$ nanobelts, which clearly indicates the presence of interstitial Na^+ ions. The XPS VB of bulk V_2O_5 (dotted line in Fig. 2) is composed of three bands, namely, bands A, B, and C located at ~3.6, 5.2, and 6.5 eV binding energies, respectively. There are no V3d electrons in bulk V_2O_5. Band A is assigned to the nonbonding oxygen lone pair or weakly bonding O2p, while bands B and C were assigned to the strong σ bonding O2p band which contain an appreciable amount of the V3d components.[10,11] The XPS VB of the $Na_2V_6O_{16}$ nanobelts (solid line in Fig. 2) is slightly different from that of bulk V_2O_5. A depletion of bands A and C was noted for the $Na_2V_6O_{16}$ nanobelts, which may imply the reduction of the V3d hybridization due to the relatively higher O/V ratio.

The FE measurements were carried out in a vacuum chamber at $\sim 8\times 10^{-7}$ torr, using a two-parallel-plate configuration with a vacuum spacing of 100 μm, as described elsewhere.[2] A conducting indium tin oxide (ITO) glass coated with a layer of phosphor was used as the anode to view the fluorescent images. Typical FE results of the $Na_2V_6O_{16}$ nanobelt papers before and after thermal annealing are shown in Fig. 3(a). It can be seen that the hydrated $Na_2V_6O_{16}\cdot 3H_2O$ nanobelt paper has a turn-on field of 7.2 V/μm and a maximal current density of 0.9 mA/cm^2 at a field of 10 V/μm. After annealing at 300 °C, the FE properties of the dehydrated $Na_2V_6O_{16}$ nanobelt paper are en-

[a)]Author to whom correspondence should be addressed; electronic mail: lin_jianyi@ices.a-star.edu.sg

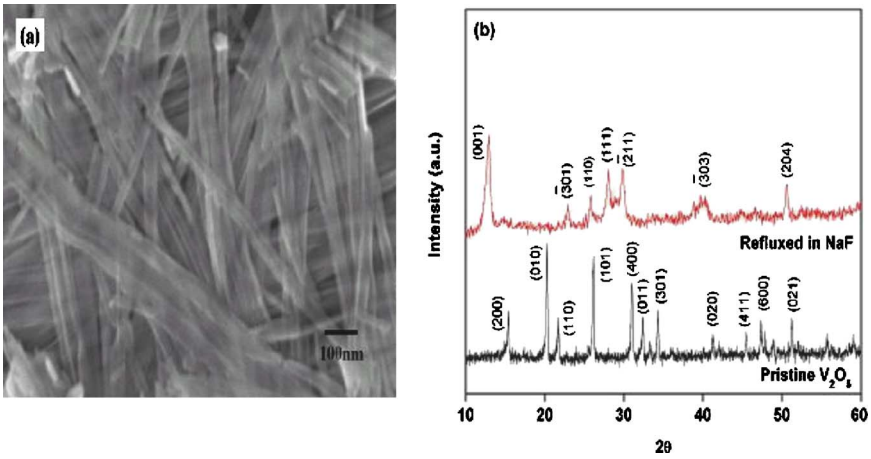

FIG. 1. (a) SEM images of dehydrated $Na_2V_6O_{16}$ nanobelts and (b) XRD profiles of the V_2O_5 samples before and after NaF reflux.

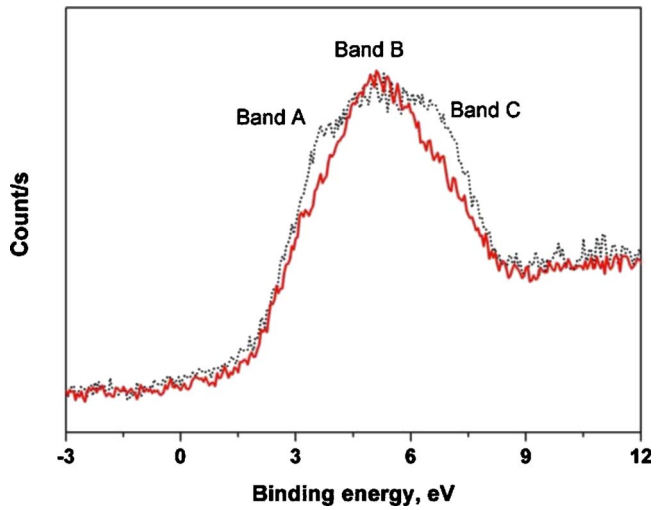

FIG. 2. XPS valence bands of dehydrated $Na_2V_6O_{16}$ nanobelts (solid red lines) and bulk V_2O_5 (dotted black lines).

hanced. The turn-on field reduces to ~6.8 V/μm and the maximal current density reaches 2.5 mA/cm^2 at the same field of 10 V/μm. It is noted that the maximal current density of the $Na_2V_6O_{16}$ nanobelts is much higher than cupric oxide nanowires[2] (0.45 mA/cm^2, 7 V/μm) and cobalt oxide nanowalls[4] (0.25 mA/cm^2, 11 V/μm), which were measured using the same experimental setup. The larger current density of $Na_2V_6O_{16}$ nanobelts might be due to its relatively higher O/V atomic ratio as investigated from the XPS valence band. Based on the Fowler-Nordheim (FN) plots [inset of Fig. 3(a)] we can see a roughly linear dependence between $\ln(J/E^2)$ and $(1/E)$ in the high field regions, which suggests a tunneling process during the electron emission. The following modified FN equation is used to analyze the FE results:[3]

$$I = \frac{A\gamma\beta^2(V-RI)^2}{\phi d^2}\exp\left(\frac{-Bd\phi^{3/2}}{\beta(V-RI)}\right) \equiv A'(V-RI)^2\exp\left(\frac{-B'}{V-RI}\right), \quad (1)$$

where I is the current, V the applied voltage, d the spacing, ϕ the work function, γ the effective emission area, β the enhancement factor, R the constant resistance of nanobelts, and A and B are constants. Parameters A' and B' in Eq. (1) can be obtained by fitting the I-V curves.[3] Thus the FE results of our samples are replotted in Fig. 3(b) with the emission current in a logarithmic scale. For the region between 500 and 700 V whereby the FN law holds best, we obtain the fitting parameters $A' = 0.000\,79 \pm 0.000\,14$ and $B' = 13\,700 \pm 150$ for

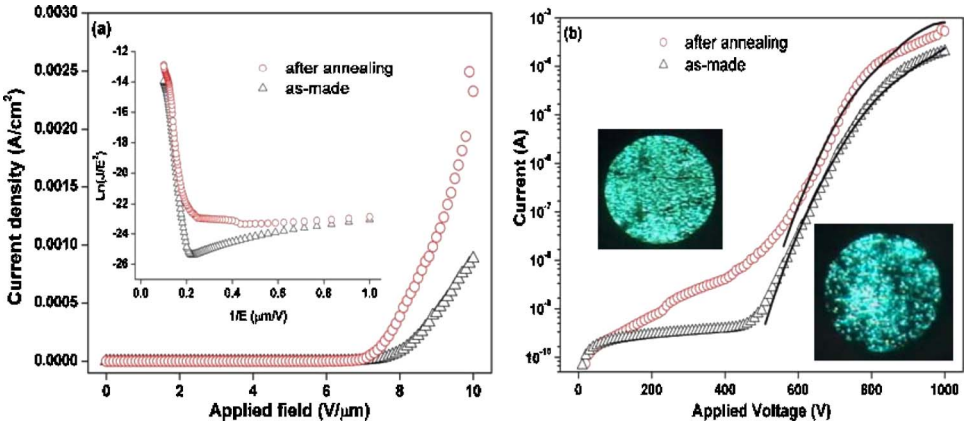

FIG. 3. (a) Field emission current-density–field (J-E) curves of hydrated $Na_2V_6O_{16}\cdot 3H_2O$) nanobelt (△△△)ss and dehydrated $Na_2V_6O_{16}$ nanobelt (○○○) paper. Inset: corresponding FN plots show roughly linear dependence. (b) Field emission current-voltage (I-V) curves plotted on semi-logarithmic scale. Black lines demonstrate the fittings using modified FN equation with an additional parameter R. Insets: fluorescent images of the hydrated (right) and dehydrated (left) nanobelt papers under a voltage of 1000 V.

the hydrated $Na_2V_6O_{16}$ sample, and $A' = 0.0022 \pm 0.0014$ and $B' = 14\,900 \pm 500$ for the dehydrated one. Both samples have a similar B' value, which suggests that they might have a similar work function. However, the dehydrated nanobelt paper has a much larger A' value, which means that the effective emission area is enhanced after thermal annealing. This is consistent with the fluorescent images [insets of Fig. 3(b)] that indicate that the number of emission sites of the $Na_2V_6O_{16}$ nanobelt paper is increased after annealing.

For $R \sim 400\ K\Omega$, the simulated curve of the hydrated $Na_2V_6O_{16} \cdot 3H_2O$ nanobelt paper can fit the measured data well up to 1000 V. On the other hand, the simulated curve for the dehydrated sample still has a slight deviation from the measured data. A best fit of R is $\sim 220\ K\Omega$ for the dehydrated nanobelt paper. We have assumed a constant R value but the resistance might increase with the rise in temperature induced by large emission current.[12] Direct two-probe measurements also indicated that the hydrated nanobelt paper had a larger resistance than the annealed sample. Therefore the annealing process helps to improve the contact between the nanobelts and reduces the resistivity of the nanobelt paper.

In summary, we have prepared crystalline $Na_2V_6O_{16} \cdot 3H_2O$ nanobelts paper via a vacuum filtration process. XPS core levels and VB studies have revealed that the dehydrated $Na_2V_6O_{16}$ nanobelts are similar to bulk V_2O_5, except for a subtle reduction in the strong O2p bonding valence band. Field emission studies have shown that dehydrated $Na_2V_6O_{16}$ nanobelt paper has a very uniform spatial distribution of the emission sites, a low turn-on field of 6.8 $V/\mu m$ and a large current density of 2.5 mA/cm^2 at an electric field of 10 $V/\mu m$.

[1] W. I. Milne *et al.*, J. Mater. Chem. **14**, 933 (2004).
[2] Y. W. Zhu, T. Yu, F. C. Cheong, X. J. Xu, C. T. Lim, V. B. C. Tan, J. T. L. Thong, and C. H. Sow, Nanotechnology **16**, 88 (2005).
[3] Y. W. Zhu, T. Yu, C. H. Sow, Y. J. Liu, A. T. S. Wee, X. J. Xu, C. T. Lim, and J. T. L. Thong, Appl. Phys. Lett. **87**, 023103 (2005).
[4] T. Yu, Y. W. Zhu, X. J. Xu, Z. X. Shen, P. Chen, C. T. Lim, and J. T. L. Thong, Adv. Mater. (Weinheim, Ger.) **17**, 1595 (2005).
[5] Y. B. Li, Y. Bando, D. Golberg, and K. Kurashima, Appl. Phys. Lett. **81**, 5048 (2002).
[6] J. Chen *et al.*, Appl. Phys. Lett. **80**, 3620 (2002).
[7] Y. Z. Jin, W. K. Hsu, Y. L. Chueh, L. J. Chou, Y. Q. Zhu, K. Brigatti, H. W. Kroto, and D. R. M. Walton, Angew. Chem., Int. Ed. **43**, 5670 (2004).
[8] B. Xiang, Q. X. Wang, Z. Wang, X. Z. Zhang, L. Q. Liu, J. Xu, and D. P. Yu, Appl. Phys. Lett. **86**, 243103 (2005).
[9] J. Yu, J. C. Yu, W. Ho, L. Wu, and X. Wang, J. Am. Chem. Soc. **126**, 3422 (2004).
[10] S. Shin *et al.*, Phys. Rev. B **41**, 4993 (1990).
[11] W. Lamberrecht, B. Djafari-Rouhani, M. Lanno, and J. Vennik, J. Phys. C **13**, 2485 (1980).
[12] N. Y. Huang *et al.*, Phys. Rev. Lett. **93**, 075501 (2004).